Articles

The Lipid-Free Structure of Apolipoprotein A-I: Effects of Amino-Terminal Deletions†

Danise P. Rogers,‡ Linda M. Roberts,§ Jacob Lebowitz,|| Geeta Datta,⊥ G. M. Anantharamaiah,⊥ Jeffrey A. Engler,*,‡ and Christie G. Brouillette*,‡,#

Department of Biochemistry and Molecular Genetics, Center for Macromolecular Crystallography, Department of Microbiology, and Department of Medicine and the Atherosclerosis Research Unit, University of Alabama at Birmingham Medical Center, University of Alabama at Birmingham, Birmingham, Alabama 35294, and the Department of Chemistry, California State University at Sacramento, Sacramento, California 95819

Received December 18, 1997; Revised Manuscript Received April 17, 1998

ABSTRACT: Deletion mutants of human apolipoprotein A-I (apo hA-I) have been produced from a bacterial expression system to explore the function of the specific domains comprising residues 1−43, 1−65, 88−98, and 187−243, respectively, in the lipid-free conformation and in the lipid-binding mechanism of apo hA-I. Initial studies on apo Δ(1−43)A-I and apo Δ(187−243)A-I have already been reported. To aid purification of these mutants, a histidine-containing N-terminal extension was incorporated (+his); in cases where comparison with the (−his) construct was possible, little effect on the physical properties due to the (+his) extension was found. All mutants have folded structures in their lipid-free state, however these structures differ widely in their relative thermodynamic stability and extent of secondary structure. The mutant with the fewest residues deleted, apo Δ(88−98)A-I(+his), has the least secondary structure (only 34% helix) and is also the least stable ($\Delta G = 2.9$ kcal/mol). Determined from sedimentation velocity measurements on the lipid-free proteins, all but apo Δ(1−65)A-I(+his) exhibited a range of conformers in solution, which fluctuated around a highly elongated species (dimensions equal to ∼(14−16) × ∼2.3 nm). Apo Δ(1−65)A-I(+his) exhibited a discrete species which was less asymmetric (dimensions equal to 9 × 2.9 nm). Apo Δ(88−98)A-I(+his) showed extreme heterogeneity with no predominating conformer. Spectroscopic studies (ANS binding and circular dichroism) indicate that there is little difference in the lipid-free structure of the carboxy-terminal deletion mutant, apo Δ(187−243)A-I(±his) compared to wild-type (wt) apo wtA-I(±his), but substantial differences are observed between wt and the amino-terminal deletion mutants, apo Δ(1−43)A-I, apo Δ(1−65)A-I(+his), and apo Δ(88−98)A-I(+his). In contrast, the lipid-binding properties are impaired for apo Δ(187−243)A-I(±his), as measured by dimyristoyl phosphatidylcholine (DMPC) liposome turbidity clearance kinetics and palmitoyloleoyl phosphatidylcholine (POPC) equilibrium binding. Apo Δ(1−43)A-I, apo Δ(1−65)A-I(+his), and apo Δ(88−98)A-I(+his) show lipid affinities statistically similar to apo wtA-I(+his), but significantly defective DMPC clearance kinetics. Interestingly, lecithin:cholesterol acyltransferase (LCAT) activation results correlate qualitatively with the lipid-binding affinity for all mutants but apo Δ(88−98)A-I(+his), suggesting that this mutant has an altered and possibly noncooperative lipid-bound structure as well as an altered lipid-free structure. These results suggest helix 1 (residues 44−65) and helix 10 (residues 220−240) are both required for native lipid-binding properties, while the presence of internal residues, at least helix 3 (residues 88−98), is essential for proper folding of both the lipid-free and lipid-bound conformations. Importantly, studies on apo Δ(88−98)A-I(+his) provide the first experimental evidence that a native-like structure is not necessary for native-like lipid affinity, but apparently is necessary for both DMPC solubilization and LCAT activation. These results provide support for a hypothetical, multistep structure-based mechanism for apo hA-I lipid binding.

Apolipoprotein (apo) A-I is the major protein of high density lipoprotein (HDL), comprising about 70% of the total HDL proteins. Human apo A-I (apo hA-I)[1] is a 243 amino acid polypeptide; residues 44−243 consist of a contiguous series of highly homologous 11-mer and 22-mer amphipathic α-helices, helices 1−10 (reviewed in ref *1*). Through largely

† Initial construction of these mutants was supported by Grant HL34343 from the National Institutes of Health. Subsequent analytical studies were supported by funds from the State of Alabama. Synthesis of oligonucleotides for site-directed mutagenesis and DNA sequencing was supported in part by NCI Grant P50 CA13148 to the UAB Comprehensive Cancer Center. Use of computer programs used for analysis of DNA sequences (from the Genetics Computer Group, Madison, WI) was supported in part by NIAID Grant P50 AI27767.

* To whom correspondence should be addressed: C.G.B. at the Center for Macromolecular Crystallography and J.A.E. at the Department of Biochemistry and Molecular Genetics.

S0006-2960(97)03112-7 CCC: $15.00
Published on Web 08/05/1998

unknown mechanisms, this unique structure endows apo hA-I with remarkably diverse functions. Structural studies of apo hA-I (reviewed in ref *2*) have been motivated by the need to understand the molecular events governing lipid metabolism and cholesterol homeostasis (reviewed in refs *3* and *4*) and also by the clinical importance of HDL (reviewed in refs *5* and *6*). HDL, quantified by its cholesterol or apo hA-I content, is the best single predictor of coronary artery disease. Accumulated in vitro and in vivo experimental evidence suggests that the negative correlation between HDL levels and the incidence of CAD is due to the role of HDL and apo hA-I in "reverse cholesterol transport" (*3*, *7*). Reverse cholesterol transport can be broken down into three steps that are exclusively assigned to HDL and, for the most part, apo hA-I function: cholesterol efflux from peripheral tissue, LCAT esterification of HDL-associated cholesterol, and receptor-mediated delivery of cholesterol ester to the liver. Apo hA-I has also been shown to possess antiinflammatory (*8*, *9*), antiviral (*10*, *11*), and antibacterial properties (*12*).

Mutagenesis has proven to be a powerful tool for studying apo hA-I (*13*−*26*). This approach has been used to identify particular regions involved in lipid and receptor binding (*15*−*20*) and LCAT activation (*17*, *18*, *20*−*23*). These studies have also sought to elucidate the lipid-bound structure of apo hA-I on discoidal rHDL particles (*19*, *20*, *24*). We have used this approach to examine the lipid-free structure of apo hA-I and to better understand the mechanism by which it binds to lipid using a variety of biochemical and structural techniques comparing native apo hA-I to mutant proteins wherein deletions of the amino-terminal 43 residues [apo Δ(1−43)A-I] or the carboxy-terminal 57 residues [apo Δ(187−243A-I] have been made (*24*−*26*). From these and other studies, we have proposed a model for lipid-free apo hA-I (Figure 6), represented by an elongated, antiparallel helical hairpin with dimensions of approximately 16 nm × 2.2 nm, which exists in a dynamic equilibrium with a more compact four helix bundle (*26*, *27*). These studies have also led us to propose that the extreme amino-terminus of apo hA-I regulates a conformational switch, by protecting a latent lipid-binding domain which becomes exposed only after the initial association of the carboxy-terminal domain with lipid (*25*).

To further explore the structural characteristics of lipid-free apo hA-I, the role of the amino-terminal residues in stabilizing the solution structure of the protein and in facilitating lipid binding has been investigated through several deletion mutants involving residues 1−98 (Figure 5). In this paper, the lipid-free structures and lipid-binding properties of these mutants have been compared with the previously described mutants, apo Δ(1−43)A-I and apo Δ(187−243)A-I (*25*, *26*). The present study demonstrates that the region defined by residues 1−98 is critical for maintaining and stabilizing the lipid-free structure of apo hA-I. In addition, the data from these mutants provides further information on the lipid-binding mechanism previously proposed (*26*).

EXPERIMENTAL PROCEDURES

Preparation of Human Apo hA-I. Human apo hA-I (apo hA-I) in the methionine-reduced state (*28*) was purified by the method of Hughes et al. (*29*), as previously described (*25*). The purified protein was stored lyophilized at −20 °C. The lyophilized protein was solubilized as needed in 8 M guanidine hydrochloride in PBS (0.02 M phosphate, and 0.15 M NaCl, pH 7.4) containing 0.02% NaN_3, and 1 mM EDTA, and subsequently dialyzed against the same buffer. An extinction coefficient of 1.13 mL/(mg·cm) at 280 nm was used to determine apo hA-I concentration in 8 M guanidine hydrochloride (*30*).

Construction of cDNA for Expression of Apo hA-I Mutants. The apo hA-I cDNA that encodes the prepropeptide form of apo hA-I (*31*) was cloned into the plasmid pGEMEX (Promega, Madison, WI) with the prepro coding region removed as described previously (*25*). To ease purification, a histidine tag, consisting of six consecutive histidines, and a Factor Xa cleavage site (New England BioLabs) were added to the amino-terminus of the apo hA-I cDNA as described elsewhere (*26*). Single-stranded DNA of this modified plasmid was prepared using standard methods (*32*) and used for site-directed mutagenesis (*33*) using the oligonucleotides 5′-CCATCACATCGAAGGTCGTCCTGTGACCCAGG-3′ (sense strand) and 5′-GGCAGGAGATGAGCCCCTACCTGGACG-3′ (sense strand) to delete nucleotide sequences encoding residues 1−65, or residues 88−98, respectively. Apo Δ(1−43)A-I and apo Δ(187−243)A-I were designed as described elsewhere (*25*, *26*). Mutants were identified by colony hybridization using the mutagenic oligonucleotide, and the sequence was confirmed by double-stranded DNA sequencing [United States Biochemical (USB), Cleveland, OH]. The mutant gene product was expressed in *Escherichia coli* BL21/DE3 cells (*34*) as described elsewhere (*25*). The harvested cells were resuspended in sterile PBS.

Purification and Characterization of Apo hA-I Mutants. The resuspended *E. coli* cell pellet was lysed by French press. The supernatant containing the recombinant protein was cleared of any particulate material and passed over a buffer-equilibrated Pharmacia Hi-Trap column as recommended by the manufacturer. The purified recombinant protein was then eluted from the column using 0.5 M imidazole. After dialysis against PBS containing 1 mM EDTA or TBS (0.02 M Tris, 0.15 M NaCl, 1 mM EDTA), the protein was checked for purity using SDS−PAGE and immunoblotting and found to be greater than 95% pure. To remove the amino-terminal histidine tag (+his), 1:50 (w/w) Factor Xa protease:protein was added to the purified protein.

‡ Department of Biochemistry and Molecular Genetics, University of Alabama at Birmingham.
§ California State University at Sacramento.
|| Department of Microbiology, University of Alabama at Birmingham.
⊥ Department of Medicine and the Atherosclerosis Research Unit, University of Alabama at Birmingham Medical Center.
Center for Macromolecular Crystallography, University of Alabama at Birmingham.

[1] Abbreviations: +his, 6x-histidine tag; ANS, 1-anilinonaphthalene-8-sulfonate; apo hA-I, human apolipoprotein A-I; CAD, coronary artery disease; CD, circular dichroism; DMPC, dimyristoyl phosphatidylcholine; EDTA, ethylendiaminetetraacetic acid; HDL, high density lipoprotein; LCAT, the plasma enzyme lecithin:cholesterol acyltransferase; NaN_3, sodium azide; PBS; phosphate-buffered saline consisting of 0.02 M phosphate, 0.15 M sodium chloride, pH 7.4; POPC, palmitoyloleoyl phosphatidylcholine; rHDL, reconstituted high density lipoproteins; TBS, Tris-buffered saline containing 0.02 M Tris, pH 7.5, 0.15 M sodium chloride and 1 mM EDTA, pH 8.0); UV, ultraviolet; vis, visible; wt, wild-type.

After cleavage, the protein mixture was passed over a Pharmacia Hi-Trap column as described above. The flow through from the column contained the cleaved recombinant protein with a native N-terminus. Amino-terminal amino acid sequencing of the recombinant protein verified that the histidine tag and Factor Xa cleavage site had been removed. Measured extinction coefficients and molecular masses obtained by SDS−PAGE, which are in agreement with those calculated from the amino acid composition, are shown in Table 1.

Lecithin:Cholesterol Acyltransferase (LCAT) Purification. The procedure of Albers et al. (*35*) was used with minor modifications. Fresh, normolipidemic human plasma was ultracentrifuged at 1.21 g/mL density. Following dialysis, the LCAT-containing fraction was subjected to Affi-Gel Blue chromatography and DE−52 chromatography. LCAT was eluted from the DE−52 column with a 75 to 200 mM NaCl gradient. SDS−PAGE showed greater than 90% purity with no apo hA-I contamination.

LCAT Activity Assay. To assess the activity of apo hA-I proteins as cofactors for LCAT, 10 μg of apolipoprotein was preincubated for 1 h at 37 °C with a constant concentration of small unilamellar vesicles of egg-derived phosphatidylcholine (45 nM) and unesterified cholesterol (10 nM), containing a trace amount of [^{3}H]cholesterol, prepared through sonication for 1 h in a 23 °C water bath (*36*), along with 1 mM EDTA, 4 mM 2-mercaptoethanol and 2.5 μg of bovine serum albumin (pH 7.4) in a total volume of 150 μL. The reaction was initiated by adding 50 μL of suitably diluted purified enzyme and incubating for 5 to 60 min at 37 °C. Free cholesterol and cholesteryl ester were separated by thin-layer chromatography on silica gel using a solvent system composed of hexane/chloroform, 2:1 (v/v). Cholesterol and cholesteryl oleate standards were visualized by immersing the TLC plate in a 3% cupric acetate, 8% phosphoric acid buffer, and then applying heat. The positions of the standards were used to determine where to cut the corresponding tritiated reaction spots, which were subsequently added to scintillation fluid and counted on a Packard Tri Carb 4530. All reactions were done in triplicate.

Binding of Apo hA-I and Apo hA-I Mutants to POPC Vesicles. The procedure of Spuhler et al. (*37*) was followed as described elsewhere (*25*). Briefly, aliquots of apolipoprotein ranging in concentration from 1 to 7 μM were vortexed and subjected to six freeze−thaw cycles with buffer-hydrated POPC (9.2 mM) over 1 h, followed by further vortexing. The resulting multilamellar vesicles were centrifuged at 4 °C for 2 h at 120000*g*. The equilibrium concentration of unbound apolipoprotein was determined from the UV spectrum of the clear supernatant. It has been previously shown (*37*) that any possible residual lipid remaining in the supernatant following centrifugation can be easily corrected for by performing the same experiment in the absence of apolipoprotein to determine the optical density of the resulting protein-free supernatant. The experimental data are best fit to a simple partition equilibrium according to eq 1:

$$X_b = K_a c_{eq} \quad (1)$$

where X_b, K_a, and c_{eq} denote the molar ratio of bound apolipoprotein to total POPC, the equilibrium binding constant, and the equilibrium concentration of unbound apolipoprotein, respectively. The slope of the linear plot of X_b versus c_{eq} is equal to K_a. The binding free energy can be calculated by eq 2. Plots of X_b versus c_{eq} are linear ($r^2 >$ 0.95) for all proteins (data not shown).

$$\Delta G = -RT \ln(55.5K_a) \quad (2)$$

Dimyristoyl Phosphatidylcholine (DMPC) Clearance. DMPC (20 mg/mL) was vortexed briefly at 27 °C in a buffer composed of 8.5% KBr, 0.01% sodium azide, 0.01% EDTA, and 0.01 M Tris, pH 7.4, as described in Pownall et al. (*38*). DMPC (1 mL, 0.5 mg/mL) was preincubated in quartz spectrophotometer cells (1 cm path length) in a thermostated (23 °C) cell compartment of a Cary 3E UV−vis spectrophotometer (Varian Australia Pty. Ltd., Victoria, Australia) for 5 min. A 0.1 mg apolipoprotein sample was transferred to the cell containing the DMPC giving a lipid:protein ratio of 5:1 (w/w). The rate of lipid−protein association was followed by monitoring the rate of clearing of lipid turbidity measured at 325 nm over a period of 8 h. The rate constants, $k_{1/2}$, were determined from a plot of log A versus time, where $k_{1/2} = 1/t_{1/2}$, and $t_{1/2}$ is defined as the time required for a 50% decrease in relative turbidity $[(A_0 - A_\infty)/A_0]$.

Boundary Sedimentation Velocity Ultracentrifugation of Apo hA-I and Apo hA-I Mutants. Boundary sedimentation velocity experiments were performed as described elsewhere (*26*, *39*) on a Beckman model XL-A analytical ultracentrifuge. The protein samples used in these experiments were homogeneous solutions containing a single detectable component of known molecular mass. Boundary sedimentation was performed using a AN60 Ti rotor at 58 000 rpm and 20 °C in either a low (60 mM ammonium bicarbonate) or a high (TBS) ionic strength buffer. Digital acquisition of the absorbance at 214 nm of the moving boundary was made at regular time intervals.

The frictional ratio of the experimental f-value divided by the frictional coefficient of either an unhydrated (f_{min}) or a hydrated sphere (f_o) of identical molecular weights can be calculated from the following equations:

$$f/f_{min} = M(1 - \bar{v}_2\rho)/Ns_{20,w}6\pi\eta[3M\bar{v}_2/4\pi N]^{1/3} \quad (3)$$

$$f/f_{min} = f/f_o(\bar{v}_2 + \bar{v}_1\Gamma'/\bar{v}_2)^{1/3} \quad (4)$$

where f/f_{min} and f/f_o are the frictional coefficient ratios due to the shape of the molecule if water is excluded (maximum asymmetry) or included, respectively, M represents the molecular mass of the protein, $\bar{v}_2$ is the calculated partial specific volume of the unhydrated protein (Table 1), N is Avogadro's number, η is the viscosity of water, ρ is the density of water, v_1 is the partial specific volume of water, and Γ' is the water of hydration expressed in grams of H_2O per gram of protein. Γ' was estimated to be 0.35 (*26*, *40*−*42*). From the calculated values of f/f_o, the maximum asymmetry can be determined for a prolate ellipsoid of revolution (*43*) using the following equation:

$$F = f/f_0 = (1 - p^2)^{1/2}/p^{2/3} \ln\{[1 + (1 - p^2)^{1/2}]/p\} \quad (5)$$

where $p = b/a = 1/p_r$; p_r is the axial ratio and F is a shape factor (Perrin factor). This asymmetry may be expressed

as the axial ratio (a/b) of the ellipsoid, where a is the radius along the long geometric axis of revolution and b is the short equatorial radius (Table 4). By using the following relationship for the molar volume of an ellipsoid:

$$M(\bar{v}_2 + \Gamma'\bar{v}_1) = 4\pi N(a/b)b^3/3 \quad (6)$$

where $\bar{v}_2$ and $\bar{v}_1$ are the partial specific volumes of the protein and solvent, respectively, and a/b is the axial ratio; the radial dimensions of the apo hA-I monomers can be determined.

Sedimentation Velocity Analysis of Apo hA-I and Apo hA-I Mutants. Van Holde and Weischet (*44*) introduced a global boundary analysis method that determines the integral distribution of s that removes boundary spreading due to diffusion. This method allows high resolution of sedimenting systems composed of multiple conformational states of a single macromolecular component (for review see ref *45*). UltraScan software developed by B. Demeler was used for the van Holde-Weischet analysis of the boundary sedimentation velocity data of native and mutant apo hA-I as described elsewhere (*26*). It can be shown that a graph of s_n* (where subscript n designates the selected boundary fraction) obtained at a fixed radial value at various times versus $t^{-0.5}$ describes a straight line. A true s* value can be obtained with extrapolation to infinite time. This method of analysis eliminates diffusion effects on boundary shape. The plots of s_n* as a function of $t^{-0.5}$ will extrapolate to an essentially single $s_{20,w}$ value for a single ideal component whereas multiple conformations for a single component will show multiple intercepts. In the van Holde-Weischet analyses, only the boundary region from 10 to 90% is used in order to eliminate noise inherent in the meniscus and the plateau.

Reversible Equilibrium Unfolding by Difference Spectroscopy. Urea-induced unfolding of lipid-free apo A-I proteins was monitored by fluorescence spectroscopy [Aminco-Bowman Series 2 fluorometer (SLM-Aminco, Rochester, NY)]. Urea stock solutions (10 M) made from Ultrapure urea (Gibco BRL, Grand Island, NY) in PBS were prepared fresh for each experiment. The concentrations of the apolipoproteins were kept constant at 0.1 mg/mL, which is below the aggregation state as assessed by Barbeau et al. (*41*) and as determined from our current studies (unpublished results). Protein samples were incubated with various concentrations of urea, ranging from 0 to 4.0 M, at 4 °C for at least 12 h to allow samples to reach equilibrium.

Fluorescence emission spectra were measured between 300 and 400 nm using an excitation wavelength of 294 nm and a bandwidth of 1 nm. The photomultiplier high voltage was kept constant during all measurements. The emission spectra were corrected by subtracting the appropriate buffer or urea blanks from the protein spectra. Difference spectra were then obtained by subtracting the protein spectra of samples containing urea from the spectrum of the protein in buffer alone. The fluorescence difference spectra (Δfluor) were analyzed at their maxima which occurred between 320 and 330 nm.

Curve Fitting of Unfolding Data. The data were fit to a two-state unfolding model (*25*, *46*). The urea-dependent equilibrium constant of unfolding, K_D, for a two-state unfolding model, can be described by eq 7:

$$K_D = \exp[(\Delta G_{H_2O} - m_D[D])/-RT] \quad (7)$$

$$f_u = K_D/(1 + K_D) \quad (8)$$

$$f_u = (\Delta y_f - \Delta y)/(\Delta y - \Delta y_u) \quad (9)$$

where ΔG_{H_2O} is the free-energy difference between the native state and the unfolded state of the protein in the absence of denaturant, [D] is the denaturant concentration, m_D is the rate of change in free energy as a function of denaturant concentration, Δy is the experimental spectroscopic measurement, and Δy_f and Δy_u are the preunfolding and postunfolding values, respectively. Equations 7 and 8 were used for global fits after converting Δfluor to f_u (the fraction of protein molecules in the unfolded state) using eq 9. $\Delta G_{H_2O}/m_D$ equals $[\text{urea}]_{1/2}$, the urea concentration at the midpoint of the unfolding transition. Δy_f and Δy_u were determined by linear regression of the first or last few data point in the unfolding curve (*25*).

1-Anilinonaphthalene-8-sulfonate (ANS)-Binding Measurements. ANS (Aldrich, Milwaukee, WI)-binding experiments were carried out on solutions containing 50 μg/mL protein and 250 μM ANS (*25*). In all cases, ANS was in at least 100-fold excess of the protein (mol/mol). ANS fluorescence was measured at an excitation wavelength of 395 nm with a 5 nm slit width. Fluorescence spectra obtained were compared to ANS in PBS alone.

Circular Dichroism Spectroscopy of Apo hA-I and Apo hA-I Mutants. The CD spectra were recorded with an AVIV 62DS spectropolarimeter which was standardized using a solution of 0.1% (w/v) *d*-10-camphorsulfonic acid. The CD spectra were measured every 0.5 nm with a 0.5 s averaging per point and a 2 nm bandwidth. A 0.01 cm path length cell was used for far-ultraviolet (UV) spectra. Spectra were signal averaged by adding at least five scans and corrected by subtracting a spectrum for the buffer alone obtained in a like manner. The spectra were normalized to molar residue ellipticity and the fraction of α-helicity in the secondary structure was estimated from the molar ellipticities at 222 nm $[[\Theta]_{222} = (-30\,300 \times f_H) - 2340]$ where f_H is the fraction of α-helical residues (*47*).

RESULTS

Apo hA-I and the apo hA-I mutants purified from *E. coli* lysates appeared homogeneous and greater than 95% pure (Figure 1). Between 40 and 120 mg of protein/L of growth media was obtained. Figure 5 illustrates the regions in apo hA-I that were deleted in the mutants described in this paper.

Factor Xa Cleavage of Lipid-Free Histidine-Tagged Apo hA-I Variants. An amino-terminal 6x histidine-tag (+his) was added to the native amino acid sequence to simplify purification of the mutant proteins. A Factor Xa cleavage site (Ile-Glu-Ser-Arg) was also engineered between the 6x histidine-tag and the amino-terminus of the protein to allow removal of the (+his) tag. In the present studies, as well as in studies by several other research groups, it is shown that the structure and function of apo hA-I and other constructs are not significantly affected by the presence of an amino-terminal extension, for example, the four residue propeptide [Phe-Trp-Gln-Gln (*23*, *48*, *49*)] and an 11 residue His-containing peptide [Met-Arg-Gly-Ser $(His)_6$-Met (*14*, *16*)]. For apo wtA-I(+his) and apo Δ(187−243)A-I(+his), the major (>90%) fragment after proteolytic digestion using

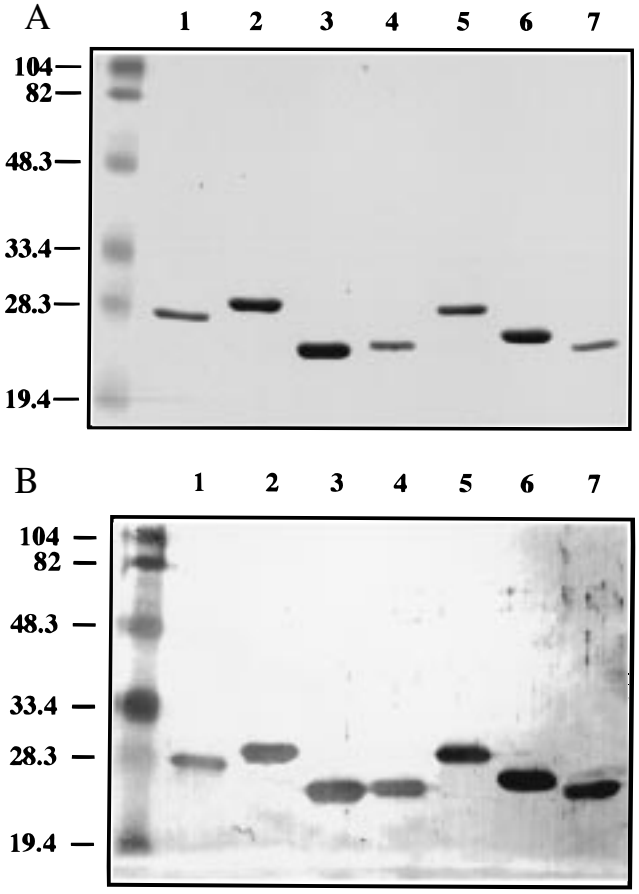

FIGURE 1: (A) SDS−PAGE analysis of purified apo hA-I and apo hA-I variants. Lane 1, apo hA-I; lane 2, apo wtA-I(+his); lane 3, apo Δ(1−43)A-I; lane 4, apo Δ(1−65)A-I(+his); lane 5, apo Δ(88−98)A-I(+his); lane 6, apo Δ(187−243)A-I(+his); lane 7, apo Δ(187−243)A-I; unlabeled lanes; molecular mass standards; molecular masses in kilodaltons are indicated. (B) Western blot analysis of apo hA-I and apo hA-I variants probed with a polyclonal antibody to apo hA-I. Lane 1, apo hA-I; lane 2, apo wtA-I(+his); lane 3, apo Δ(1−43)A-I; lane 4, apo Δ(1−65)A-I(+his); lane 5, apo Δ(88−98)A-I(+his); lane 6, apo Δ(187−243)A-I(+his); lane 7, apo Δ(187−243)A-I; unlabeled lanes; molecular mass standards; molecular masses in kilodaltons are indicated.

factor Xa is the recombinant protein with a native amino-terminus, e.g., D-E-P-P-Q (Table 2). However, for apo Δ(1−65)A-I(+his) and apo Δ(88−98)A-I(+his), limited proteolysis resulted in two and three major fragments, respectively (Table 2). For apo Δ(1−65)A-I(+his), none of the fragments contained the expected amino-terminal sequence, P_{65}-V-T-Q-E; instead cleavage sites were identified at Q_{132} in helix 5, at A_{154} in helix 6, and E_{224} in helix 10 [Q_{132} and E_{224} are near cleavage sites seen in lipid-free apo hA-I (*27*)]. This suggests the structural arrangement of helices has been altered such that (1) the engineered cleavage site is no longer accessible to proteolytic attack and (2) additional cleavage sites have become exposed. For apo Δ(88−98)A-I(+his), the engineered amino-terminal site was accessible for cleavage; however, peptide sequencing indicated two additional cleavages occurred at Q_{132} in helix 5 and A_{154} in helix 6. It is interesting that these two mutants have the least stable lipid-free structures by urea unfolding, suggesting that their increased susceptibility toward cleavage at two sites that are susceptible to cleavage in the native protein may be related to their thermodynamic stability. For better comparison among the mutants, all studies were carried out with the (+his) recombinant proteins. Apo hA-I and apo Δ(187−243)A-I served as (−his) controls, and as shown in Figure 2 and Tables 3, 4, and 5, the properties of each pair of (±his) proteins are statistically the same.

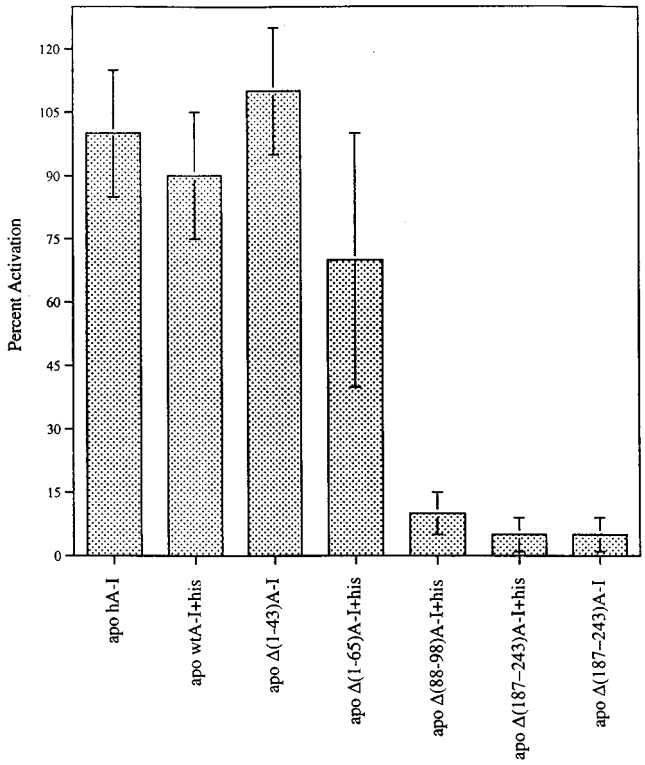

FIGURE 2: Activation of LCAT by apo hA-I and mutants using a vesicular assay. The bar graph data (± standard deviation) represent the percent activation relative to apo hA-I (activation = 100%).

Lipid-Binding Properties of Apo hA-I and Apo hA-I Mutants. The lipid-associating ability of apo hA-I proteins was assessed by two different methods, POPC equilibrium binding and kinetics of DMPC liposome turbidity clearance. A POPC vesicular binding assay (*37*) was used to estimate the lipid-binding free energies for the apo hA-I proteins (Table 3), a method we have previously applied to apo Δ(1−43)A-I (*25*). The lipid-binding free energies are similar ($p < 0.05$) for apo hA-I, apo wtA-I(+his), apo Δ(1−43)A-I (*25*), and apo Δ(88−98)A-I(+his). Apo Δ(1−65)A-I(+his) has less lipid affinity than apo hA-I and apo wtA-I(+his), although the latter was on the border of statistical significance. Apo Δ(187−243)A-I(±his) has a significantly lower affinity.

The rates of association of apo hA-I proteins were determined by measuring the rate of clearance of DMPC liposomal turbidity. Binding to DMPC liposomes results in a conformational rearrangement of protein and lipid that disrupts or "solubilizes" the DMPC liposomes, producing small discoidal micelles. All mutants show slower kinetics than intact apo hA-I(±his) (Table 3), but apo Δ(88−98)A-I(+his) was seriously deficient and apo Δ(187−243)A-I(±his) clearance was barely perceptible, as previously reported for a similar carboxy-terminally truncated apo hA-*I* (*20, 50*).

LCAT Activation. The ability of the apo hA-I proteins to serve as cofactors for LCAT was determined by measuring the initial velocity of the LCAT reaction using an egg PC vesicular assay (Figure 2). As performed, the assay does

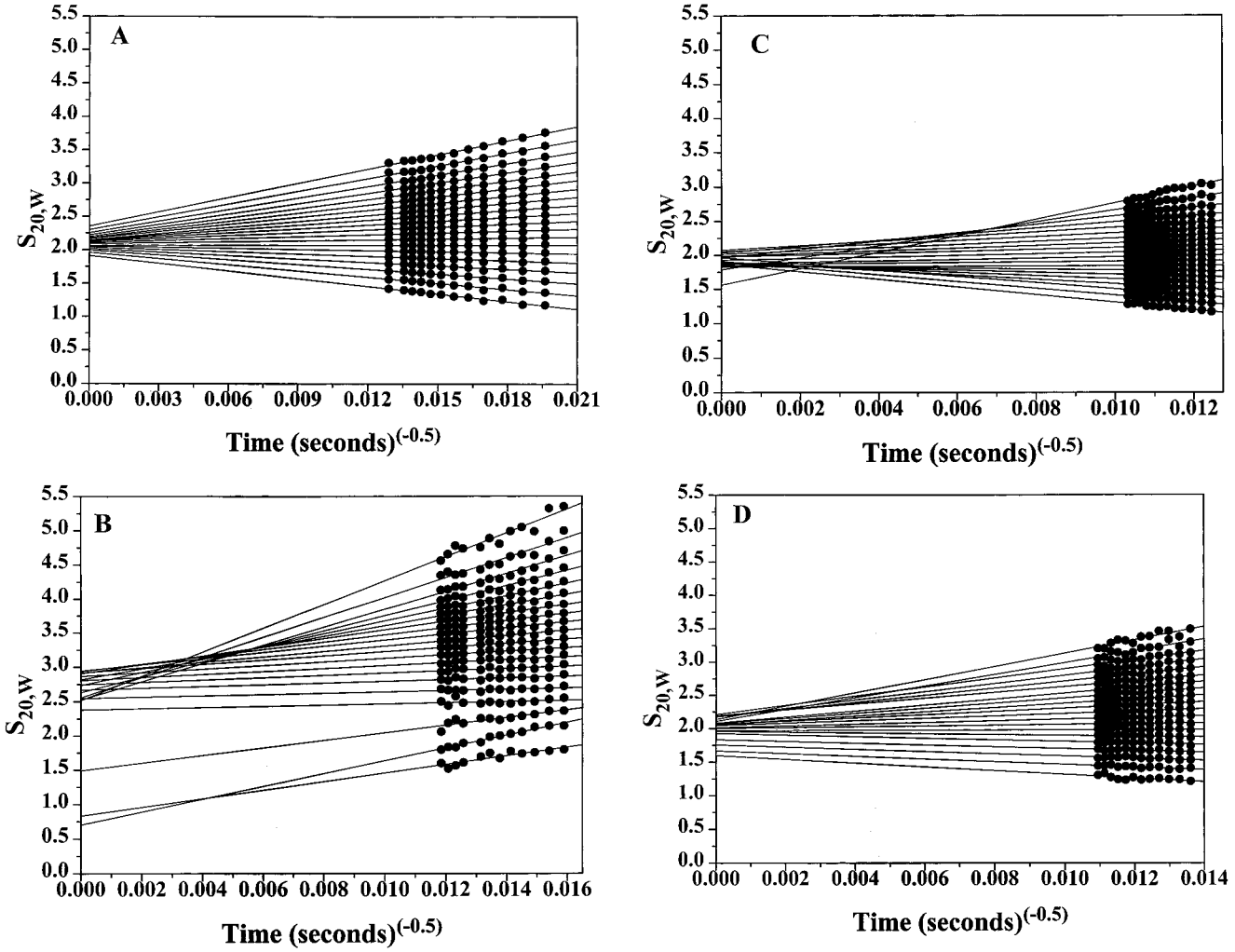

FIGURE 3: Representative van Holde-Weischet extrapolation plots of (A) apo Δ(1−65)A-I(+his), (B) apo Δ(88−98)A-I(+his), and (C) apo Δ(187−243)A-I(+his), and (D) apo hA-I. Plots for apo Δ(187−243)A-I and apo Δ(1−43)A-I can be found in (*26*). This analysis of a one-component system indicates multiple *s*-values exist, consistent with an equilibrium of monomeric conformers at low concentrations (0.1 mg/mL) of the protein (Table 4).

not distinguish between poor lipid binding and the inability to activate LCAT. Therefore, as anticipated, apo Δ(1−43)A-I and apo Δ(1−65)A-I(+his) had LCAT activation properties more similar to native apo hA-I than apo Δ(187−243)A-I(±his), which was marginal as a cofactor (consistent with its reduced lipid affinity). Activation studies using a similar carboxy-terminal deletion of apo hA-I indicated that the carboxy-terminal domain, while affecting the lipid-association properties of the protein, does not affect its intrinsic ability to serve as a cofactor for LCAT (*50*). Unexpectedly, apo Δ(88−98)A-I(+his) exhibited only 10% of native apo hA-I activity, a difference which cannot be explained by a lower affinity for lipid (Table 3).

Boundary Sedimentation Velocity. The method of van Holde and Weischet (*44*) was used to analyze sedimentation velocity data obtained for each mutant protein. The experimental data are shown in Figure 3 and are summarized in Table 4; similar data for two other mutants, apo Δ(1−43)A-I and apo Δ(187−243)A-I, were determined previously (*26*). The *y*-intercepts (Figure 3) correspond to infinite time and yield the diffusion-corrected s_n* of each boundary fraction. Frictional ratios, f/f_{min} and f/f_o, were calculated using eqs 3 and 4. All proteins but apo Δ(1−65)A-I(+his) exhibit a discrete range of *s** values, suggesting the existence of a dynamic conformational heterogeneity, a phenomenon which becomes more pronounced when the ionic strength of the buffer is lowered [Table 4 (*45*)]. On the other hand, the *average* frictional ratios for all but apo Δ(88−98)A-I(+his) remain essentially the same over the range of buffers used (Table 4). The van Holde−Weischet profile suggests that apo Δ(88−98)A-I(+his) exists in many different, interconvertible conformations, with no preference for any one arrangement, which is consistent with a very unstable, noncooperative tertiary structure.

Assuming a prolate ellipsoid and a hydration of 0.35 g of H_2O/g of protein, the axial ratios (*a*/*b*) due to asymmetry were estimated (Table 4). These ratios indicate that all apo hA-I monomers are highly asymmetric, exhibiting similar average dimensions for all but apo Δ(1−65)A-I(+his) (which is less asymmetric) and apo Δ(88−98)A-I(+his) (Table 4). For all but the exceptions, the data support a dynamic equilibrium between a four helix bundle and an elongated monomeric helical hairpin (Figure 6). For apo Δ(88−98)A-I(+his), the entire range of axial ratios was estimated to be from 1.0 to >15, however, the higher axial ratios ($a/b > 7$) probably represent multimeric aggregates of the mutant protein.

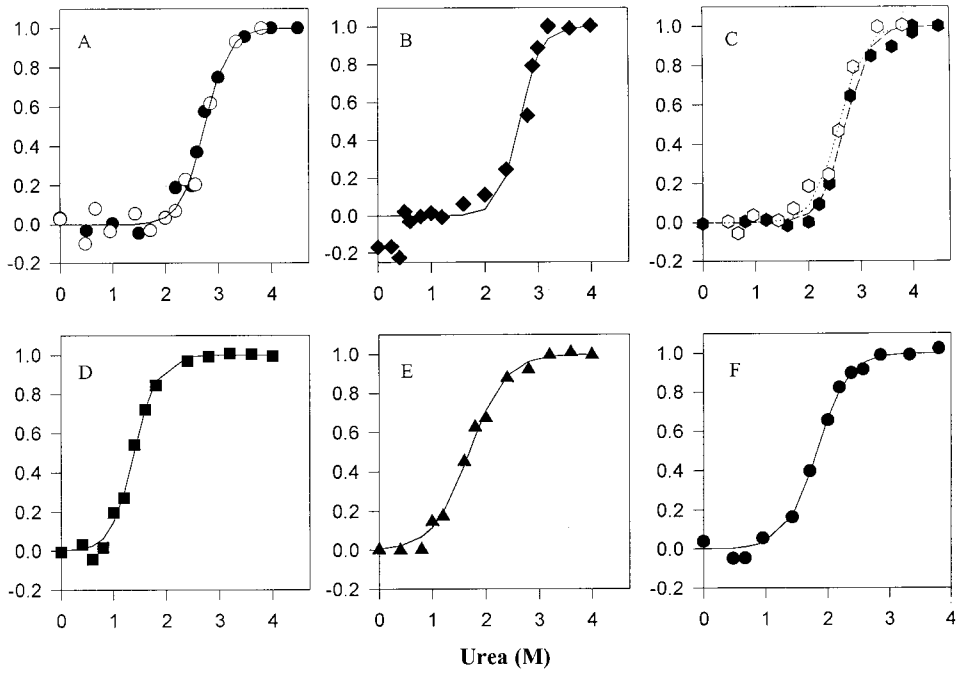

FIGURE 4: Urea-induced unfolding of (A) apo hA-I [open circles (*25*) fluorescence unfolding only, and closed circles], (B) apo wtA-I(+his) (diamond), (C) apo Δ(187−243)A-I [open hexagon, dotted line (*26*) fluorescence unfolding only] and apo Δ(187−243)A-I(+his) (closed hexagon, solid line), (D) apo Δ(1−43)A-I [square (*25*) fluorescence unfolding only], (E) apo Δ(1−65)A-I(+his) (triangle), and (F) apo Δ(88−98)A-I(+his) (closed circle) monitored by fluorescence emission. The experimental data are normalized to the apparent fraction of unfolded protein, f_u, as a function of urea concentration. Symbols represent unfolding experiments and the solid lines represent two-state fits through the data for each protein to determine a single set of thermodynamic parameters (Table 5).

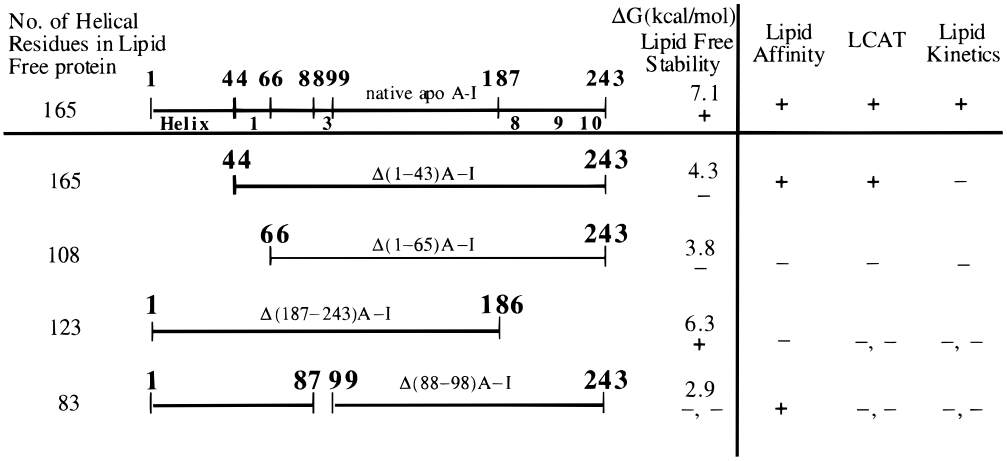

FIGURE 5: A summation of the helicity, stability, lipid binding and LCAT activation data for each of the deletion mutants compared to apo hA-I. The various apo hA-I proteins are indicated in the left panel with the respective deletions depicted; helices which have been deleted are numbered in the linear map of apo hA-I at the top. The number of helical residues based on CD (Table 3) are shown in the first column (far left panel) and the relative stabilities, ΔG_{H_2O}, of the proteins, calculated from urea-induced unfolding (Table 3) are indicated in the third column (left panel). The right panel gives the relative results of the proteins ability to bind to POPC vesicles (Table 3), their ability to activate LCAT (Figure 2), and their ability to break down DMPC multilamellar vesicles into smaller micelles (Table 3), respectively. (+) Positive result that is statistically similar to that observed for apo hA-I. (−) Result which is statistically lower than apo hA-I. (−,−) indicates a negative result.

Spectral Properties of Lipid-Free Apo hA-I Variants. Far-UV (222 nm) circular dichroism was used to compare the relative secondary structures of the lipid-free forms of the apo hA-I proteins from which an estimate of the number of α-helical residues was derived (Table 3). Only apo Δ(88−98)A-I(+his) shows a significant decrease in α-helicity which cannot be explained solely by the decrease in number of amino acid residues.

When the apolar, fluorescent dye, ANS, binds to apo hA-I, both enhanced fluorescence and a shift in the wavelength of peak emission (λ max) from a maximum at 515 nm (*51*) toward lower wavelengths are observed for all of the apo hA-I proteins (Table 5). Thus, all of the proteins bind ANS, presumably to an exposed hydrophobic surface or cavity (*52*). As a negative control, no change in fluorescence is associated with the addition of ANS to carbonic anhydrase (λ_{max} at 515 nm), a stabley folded globular protein of similar size (*53*).

Measurements of Reversible Equilibrium Unfolding by Spectroscopy. Denaturation of apo hA-I proteins with urea was monitored using fluorescence emission difference spectroscopy. In all cases, the unfolded proteins exhibit lower fluorescence intensities with concomitant red shifts of the

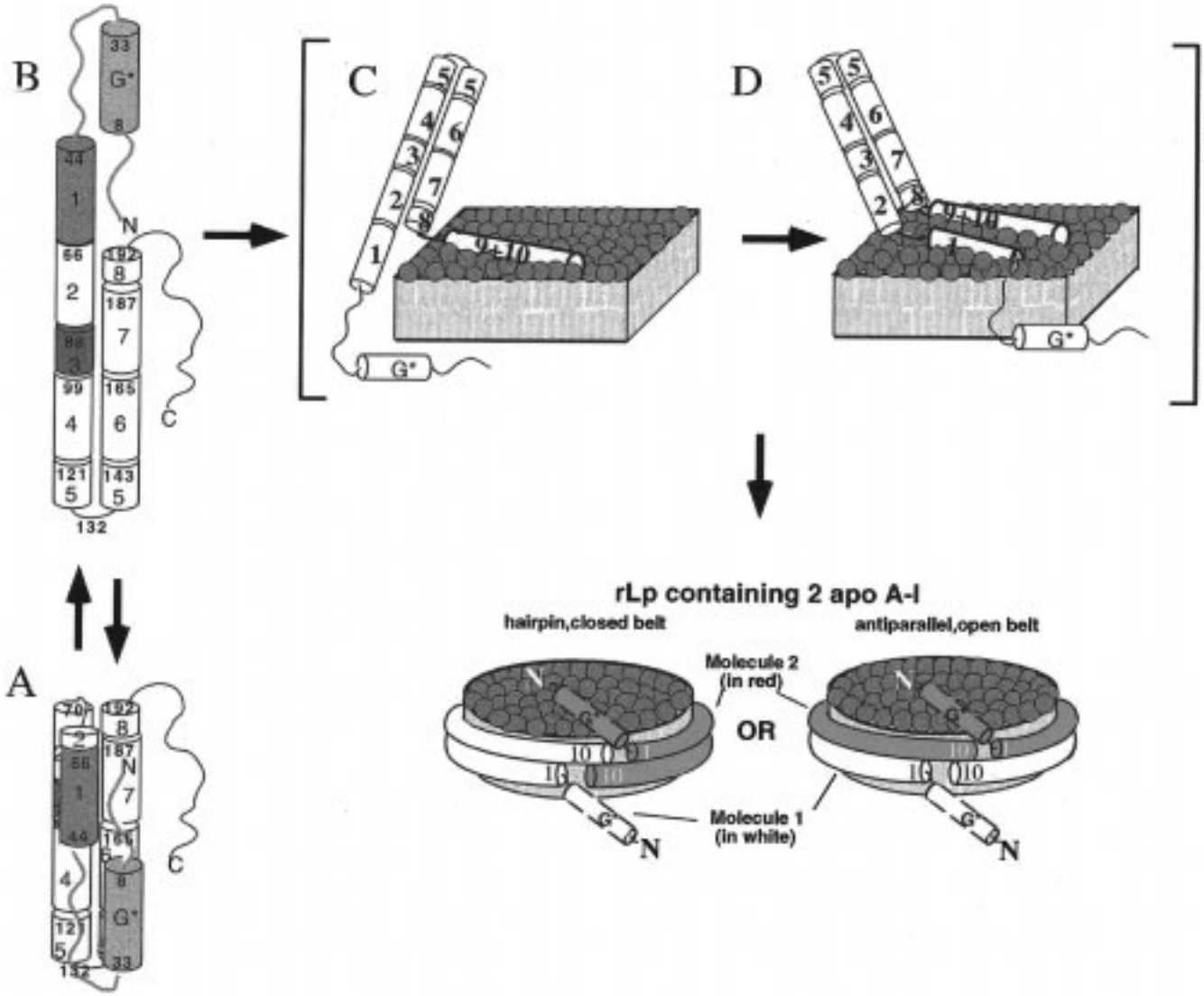

FIGURE 6: Hypothetical structure-based lipid binding mechanism for apo hA-I. (A) Proposed tertiary structural model of lipid-free apo hA-I, depicting a folded helical bundle adapted from refs *26* and *27*; (B) the elongated monomeric helical hairpin derived from analytical ultracentrifugation (*26*, *41*). The purple shaded regions represent those deleted in the mutants studied here. Helices are numbered according to the repeating sequence homology (*1*, *2*). (C) The initial lipid binding step of lipid-free apo hA-I mediated through a largely unfolded and uncooperative carboxy-terminal domain. Binding of these residues is associated with an increase in the overall α-helicity of the protein. (D) Later intermediate produced following a conformational switch of residues 1−43 which unmasks a latent lipid-binding domain, most likely represented by the residues of helix 1 (amino acids 44−65). Final products are depicted here as discoidal lipoproteins containing 2 apo hA-I molecules. The perpendicular orientation relative to the acyl chains of the lipids is suggested by the crystal structure of apo Δ(1−43)A-I (*24*).

Table 1: Amino Acid Compositions and Molecular Masses of Apo hA-I and Apo hA-I Mutants

apolipoprotein	no. of amino acids	molecular mass[a] (kDa)	extinction coefficient[b] (ϵ_{280}) (mL/mg·cm)
apo hA-I	243	28.1	1.13
apo wtA-I(+his)	254	29.6	1.07
apo Δ(1−43)A-I	201	23.3	0.992
apo Δ(1−65)A-I(+his)	189	22.2	0.81
apo Δ(88−98)A-I(+his)	243	28.3	1.12
apo Δ(187−243)A-I(+his)	199	23.1	1.325
apo Δ(187−243)A-I	188	21.7	1.24

[a] Molecular Mass calculated on the basis of the amino acid composition. See Figure 1. [b] Determined at 280 nm in 8 M guanidine hydrochloride.

peak wavelength, indicating an increase in the polarity of the environment surrounding the tryptophans due to the unfolding of the native structure.

As previously performed on apo Δ(1−43)A-I and apo Δ(187−243)A-I, a two-state model was used with a global fit of all spectral unfolding curves for each proteins yielding the parameters ΔG_{H_2O}, m_D, and $[\text{urea}]_{1/2}$ (Figure 4 and Table 5). The experimental values obtained from the urea-induced unfolding of apo hA-I compared to apo Δ(187−243)A-I(±his) are not significantly different, suggesting that the carboxy-terminus does not play a major role in the stability of the protein, as previously reported for the (-his) construct [Table 5 (*26*)]. However, as reported for apo Δ(1−43)A-I, the deletion of the extreme amino-terminus has a profound effect on the stability of the protein compared to apo wt A-I(+his) [$\Delta G_{H_2O} = 3.75 \pm 0.28$ kcal/mol and 4.27 ± 0.30 kcal/mol for apo Δ(1−65)A-I(+his) and apo Δ(1−43)A-I, respectively]. Interestingly, the additional deletion of helix 1 (residues 44−65) does not appear to have a major impact on the stability of the protein to unfolding relative to apo

Table 2: Limited Proteolysis of Histidine-Tagged Apo A-I Mutants Using Factor Xa

apo Δ(1−65)A-I(+his)		apo Δ(88−98)A-I(+his)		apo Δ(187−243)A-I(+his)		apo wtA-I(+his)	
MW[a]	protein sequence[b]	MW[a]	protein sequence[b]	MW[a]	protein sequence[b]	MW[a]	protein sequence[b]
22.2[c]	$(M_{-11}\text{-}R_{-1})P_{66}\text{-}Q_{243}$[d]	27.8[c]	$(M_{-11}\text{-}R_{-1})D_1\text{-}Q_{243}$[f]	22.5[c]	$(M_{-11}\text{-}R_{-1})D_1\text{-}G_{186}$	29.2	$(M_{-11}\text{-}R_{-1})D_1\text{-}Q_{243}$
9.3	$(M_{-11}\text{-}R_{-1})P_{66}\text{-}R_{131}$[d]	26.8[e]	$D_1\text{-}Q_{243}$[f]	21.5[e]	$D_1\text{-}G_{186}$	28.1	$D_1\text{-}Q_{243}$
8.2	$A_{154}\text{-}L_{223}$	15.2	$(M_{-11}\text{-}R_{-1})D_1\text{-}R_{154}$[f]				
		12.5	$(M_{-11}\text{-}R_{-1})D_1\text{-}L_{122}$[f]				

[a] Molecular Mass of the peptide expressed in kilodaltons. [b] The sequence of resultant peptide after cleavage with Factor Xa as determined from N-terminal sequencing and molecular mass. [c] This represents the native protein sequence before cleavage. [d] Sequence in parentheses represents the histidine-tag and the Factor Xa cleavage sequence. [e] This represents the native protein sequence after cleavage. [f] Native sequence does not include residues 88−98.

Table 3: Lipid-Binding Properties and Helicity of Apo hA-I and Apo hA-I Amino-Terminal Variants

apolipoprotein	Δ*G* of binding[a] (kcal/mol)	DMPC clearance $k_{1/2}$ (min^{-1})	% α-helix[b]	helical aa[c]
apo hA-I	−5.13 ± 0.14	0.89 ± 0.12	68 ± 4	165
apo wtA-I(+his)	−4.78 ± 0.13[d]	0.690 ± 0.034[d]	nd	nd
apo Δ(1−43)A-I	−4.82 ± 0.09[d,e]	0.40[f]	68 ± 5	165
apo Δ(88−98)A-I(+his)	−5.08 ± 0.08[d,e]	0.105 ± 0.008[f]	34 ± 2	83
apo Δ(1−65)A-I(+his)	−4.51 ± 0.21[e,h]	0.488 ± 0.016[f]	57 ± 4	108
apo Δ(187−243)A-I(+his)	−4.33 ± 0.15[f,g]	0.027 ± 0.008[f,g]	62 ± 4	123
apo Δ(187−243)A-I	−4.26 ± 0.12[f,g]	0.042[f,g]	82 ± 2	127

[a] Δ*G* of binding to POPC vesicles was calculated by eq 2 in the Experimental Procedures. [b] Percent helix was estimated by the method of Chen et al. (*47*). [c] The number of helical amino acids (aa) in the protein are estimated by multiplying the fractional helicity by the number of residues in the protein (see Table 1). [d] A Student's *t*-test indicates the values for native apo hA-I and recombinant protein are statistically the same ($p < 0.05$). [e] A Student's *t*-test indicates the values for apo wtA-I(+his) and the amino-terminal mutants indicated are statistically the same ($p < 0.05$). [f] A Student's *t*-test indicates the values for apo wtA-I(+his) and the mutants indicated are statistically not the same ($p > 0.05$). [g] A Student's *t*-test indicates the values for apo Δ(187−243)A-I(±his) are statistically the same ($p < 0.05$). [h] The lower Δ*G* compared to apo Δ(1−43)A-I and apo wtA-I(+his) is on the border of statistical significance at $p \approx 0.05$. Standard deviations are reported where at least two different experiments were performed; up to four experiments and up to three preparations of each protein were used in these experiments.

Table 4: Sedimentation Velocity Properties of Apo hA-I and the Amino-Terminal Apo hA-I Mutants

apolipoprotein/MW	$\bar{v}_2$[e]	$s_{20,w}a$	f/f_{min}	f/f_0	a/b[b]	molecular dimensions (nm), $2a \times 2b$
apo hA-I	0.735	2.06 ± 0.23	1.58	1.39	7.2	
28 303			(2.49−1.3)[c]	(2.18−1.10)[c]		16.8 × 2.4[f,h]
			1.58	1.39		
		2.04 ± 0.09	(1.75−1.51)[d]	(1.54−1.32)[d]	7.2	
apo Δ(1−65)A-I(+his)	0.738	2.21 ± 0.17	1.24	1.09	3.1[c]	
22 249		2.12 ± 0.03	(1.52−1.15)[c]	(1.33−1.01)[c]		9.0 × 2.9
			1.29	1.13	3.1[d]	
			(1.34−1.24)[d]	(1.17−1.09)[d]		
apo Δ(88−98)A-I(+his)	0.734	2.42 ± 0.62	(4.42−1.12)[c]	(3.92−1.0)[c]	range of	range of (4.6 × 4.6)−
28 314		2.18 ± 0.68	(4.41−1.14)[d]	(3.87−1.0)[d]	1.0−6.2[g]	(13.4 × 2.2)[g]
apo Δ(187−243)A-I(+his)	0.731	1.91 ± 0.09	1.51	1.32	6.2[c]	
23 073			(1.83−1.42)[c]	(1.61−1.25)[c]		14.2 × 2.4
		1.94 ± 0.06	1.48	1.3	6.0[d]	
			(1.65−1.40)[d]	(1.45−1.23)[d]		
apo Δ(1−43)A-I	0.738	1.76 ± 0.29	1.54	1.35	6.8	15.6 × 2.3[h]
23 353			(2.33−1.06)[c]	(2.04−0.93)[c]		
		2.06 ± 0.13	1.58	1.37	7.0	
			(1.38−1.08)[d]	(1.21−0.95)[d]		
apo Δ(187−243)A-I	0.731	1.69 ± 0.25	1.54	1.35	6.8	
21 601			(1.96−1.28)[c]	(1.71−1.12)[c]		15.0 × 2.22[h]
		1.78 ± 0.20	1.54	1.35	6.8	
			(1.90−1.31)[d]	(1.67−1.15)[d]		

[a] The average $s_{20,w}$ value ± the standard deviation from two to five experiments in which the ionic strength of the buffer was varied. [b] The axial ratio calculated (*43*) for apo hA-I and the mutants based on the f/f_0 assuming a prolate ellipsoid (*41*, *60*). [c] The range of values calculated for the proteins in a low ionic strength buffer. [d] The range of values calculated for the proteins in a high ionic strength buffer. [e] Calculated using UltraScan data analysis software package developed by B. Demeler based on Cohn et al. (*61*). [f] This result is identical to the dimensions cited by Barbeau et al. (*41*). [g] The dimensions for apo Δ(88−98)A-I(+his) have no major species and vary depending on the *a*/*b* ratio. Accordingly, no average was calculated (see Figure 3; panel B). [h] These values are reported for comparison (*26*).

Δ(1−43)A-I. Significant structural instability was also observed with apo Δ(88−98)A-I(+his). Although this mutant contains an intact extreme amino-terminus, the observed ΔG_{H_2O} was only 2.94 ± 0.21 kcal/mol, less than half of the value obtained for apo hA-I.

DISCUSSION

Our focus has been to study the lipid-free structure of apo hA-I using deletion mutants to define how particular structural elements, the amphipathic α-helical segments,

Table 5: Thermodynamic Parameters of Folding for Apo hA-I and Apo hA-I Variants

apolipoprotein	ΔG_{H_2O} (kcal/ mol)	m_D (kcal mol^{-1} M^{-1})	$[urea]_{1/2}$ (M)	relative fluorescence intensity[a]
apo hA-I	7.07 ± 0.65[c]	2.57 ± 0.24[f]	2.7	1.0
apo wtA-I(+his)	7.87 ± 1.87[c]	2.96 ± 0.67[f]	2.7	1.47[b]
apo Δ(1−65)A-I(+his)	3.75 ± 0.28[d]	2.70 ± 0.20[f]	1.4	1.88
apo Δ(88−98)A-I(+his)	2.94 ± 0.21[e]	1.74 ± 0.12[g]	1.7	0.73
apo Δ(187−243)A-I(+his)	6.82 ± 0.63[c]	2.52 ± 0.23[f]	2.7	0.53
apo Δ(1−43)A-I	4.27 ± 0.30[d]	2.33 ± 0.16[f]	1.84	2.79
apo Δ(187−243)A-I	6.26 ± 0.29[c]	2.43 ± 0.11[f]	2.6	0.53

[a] ANS binding fluorescence intensities have been normalized to previously reported data (*26*). [b] One possible explanation for the differences in ANS binding between apo hA-I and apo wtA-I(+his) is electrostatic interactions between ANS and the 6x-his-tag of apo wtA-I(+his). Tryptophan 8 is near the amino-terminal his tag and may form the nidus of a hydrophobic pocket for ANS association. This proposal is consistent with the pretransition observed in the urea-induced unfolding of apo wtA-I + his observed by intrinsic fluorescence difference spectroscopy (see Figure 4). [c] A Student's *t*-test indicates these values for native apo hA-I and the indicated recombinant proteins are statistically the same ($p < 0.05$). [d] A Student's *t*-test indicates these values for apo Δ(1−43)A-I and apo Δ(1−65)A-I(+his) are statistically the same ($p < 0.05$) but are statistically different from apo hA-I and apo wtA-I(+his) ($p > 0.05$). [e] A Student's *t*-test indicates this value is statistically different from apo hA-I and apo wtA-I(+his) ($p > 0.05$). [f] A Student's *t*-test indicates these values for native apo hA-I and the indicated recombinant proteins are statistically the same ($p < 0.05$). [g] A Student's *t*-test indicates this value is statistically different from apo hA-I and apo wtA-I(+his) ($p > 0.05$).

serve specific functional roles in the mechanism(s) for lipid binding. Previously, we showed that the amino-terminal 43 residues, but not the carboxy-terminal 56 residues, are important for maintaining the structural integrity of the lipid-free protein and used this information, along with limited proteolysis data, to propose a structural model of lipid-free apo hA-I (*25*−*27*). In the present paper, we report the results of studies on several additional mutants, particularly the amino-terminal deletion mutants apo Δ(1−65)A-I(+his) and apo Δ(88−98)A-I(+his), to further define the lipid-free structure of apo hA-I and to identify those regions important for function, as determined by lipid binding and LCAT activation (a summary of experimental results is shown in Figure 5).

Lipid-Free Structures of Apo hA-I Mutants. While little difference has been observed between the lipid-free structures of apo hA-I and apo Δ(187−243)A-I(±his) (*25*, *26*), substantial differences in conformation are observed for the amino-terminal deletion mutants apo Δ(1−43)A-I, apo Δ(1−65)A-I(+his), and apo Δ(88−98)A-I(+his). We have suggested previously that the extreme amino-terminus (residues 1−43) serves as a necessary structural component in the lipid-free conformation of apo hA-I (*25*−*27*).

Further truncation of the amino-terminal region through residue 65 seems to leave the remaining structure in a similar conformation to that of apo Δ(1−43)A-I, based on most of the properties studied here with the exception of the sedimentation velocity results. Interestingly, the latter studies suggest that apo Δ(1−65)A-I(+his) does not exhibit the conformational dynamics of the other proteins, but exists in predominantly a single conformer with intermediate asymmetry. The decrease in the number of helical residues for this mutant (Table 5) directly corresponds to the deletion of residues 44 through 65, while ANS binding and ΔG_{H_2O} are more similar to the values exhibited by apo Δ(1−43)A-I. Thus, we conclude that loss of helix 1 (residues 44−65), beyond the loss of residues 1−43, results in only a small further perturbation of the lipid-free structure.

Apo Δ(88−98)A-I(+his), which contains an intact extreme amino-terminus, shows dramatic decreases not only in the stability of the molecule, but also in the helicity (a 5% loss in the number of amino acids due to the deletion compared to a 50% loss in α-helicity). These results indicate that apo Δ(88−98)A-I(+his) has a largely unfolded and uncooperative structure. In addition, the decrease in ANS binding supports a highly unstable structure, more similar to an unfolded protein rather than the highly plastic nature associated with apo hA-I. Taken together, these results suggest that helix 3 is required for directing and/or orienting the native folding pattern and helical associations of apo hA-I.

All deletion mutants so far studied are shown here to be highly asymmetric in solution and to exist in a dynamic equilibrium of conformers, consisting of at least three average conformational states, two of which are represented in Figure 6 for apo hA-I: (1) a globular helical bundle with average dimensions of 9 nm × 2.9 nm (species A, Figure 6), (2) an elongated monomeric helical hairpin with average dimensions of 16 nm × 2.4 nm (species B, Figure 6), and (3) multimeric aggregates (not shown). Apo Δ(88−98)A-I(+his) may possess additional conformations, due to its highly unstable structure. The range of conformers identified by analytical ultracentrifugation represents a highly plastic apo hA-I molecule, which is consistent with its role in lipid binding and may be relevant to the diversity of function ascribed to it.

Apo Δ(88−98)A-I(+his) is the first apo hA-I mutant representing the deletion of internal residues for which a dramatic effect on structure has been reported. It is not surprising that a deletion of as little as 11 residues would result in a major structural alteration if the residues are part of the core-folded structure rather than an external loop. This result contrasts with three separate internal deletions of 43 residues, respectively, representing deletion of helices 4 + 5, 5 + 6, and 6 + 7 (collectively encompassing residues 100−186), which had little effect on the helicity and thermodynamic stability of the lipid-free state (*16*).

Lipid-Binding Properties of Apo hA-I Mutants. The similarity in physical and spectral properties seen for lipid-free apo Δ(1−65)A-I(+his) and apo Δ(1−43)A-I is carried over to similar, lipid-binding and LCAT activation properties. The small decrease in POPC binding observed for apo Δ(1−65)A-I(+his) relative to apo Δ(1−43)A-I may be explained by the loss of a small region of the protein with high lipid-binding affinity. Studies with synthetic peptides indicate that, of the 10 putative amphipathic helices, helices 1 (residues 44−65) and 10 (220−241) have the highest affinity for lipid (*54*) and our studies on the amino- and carboxy-terminal deletion mutants support the importance of their role in the

lipid affinity of intact apo hA-I (*15*, *18*, *20*, *50*, *55*).

Apo Δ(88−98)A-I(+his) contains both helices 1 and 10 and has native-like lipid affinity. However, the dramatic loss in secondary structure and thermodynamic stability of the lipid-free state seems to be reflected in a reduced ability to solubilize DMPC. Also, a decrease in LCAT activation is observed that may be due to a structural alteration of the lipid-bound state. The ability of this mutant to bind POPC is the first direct experimental evidence that a cooperative and stable structure is not necessary for lipid affinity, but apparently *is* necessary for both DMPC solubilization and LCAT activation. These apolipoproteins must undergo a significant structural reorganization to bind to lipid. While the particulars of the conformational transition(s) required for LCAT activation and micellar formation are unknown, perhaps they are related. The required cooperativity for either function may also be an inherent property of the lipid-free structure, as the results for apo Δ(88−98)A-I(+his) suggest.

Lipid-Binding Mechanism For Apo hA-I. With all the structural data on mutants obtained to date, we suggest a structure-based mechanism for apo hA-I lipid binding (Figure 6). Sedimentation velocity experiments directly support the presence of a range of conformers which interconvert between the two extremes represented by species A and B. The dimensions of these molecular models are consistent with the ranges presented in Table 4. The intrahelical interactions suggested in the globular structure, species A, (previously presented in ref *27*) and the hairpin structure, species B, are precisely those found between molecules in our crystal structure of apo Δ(1−43)A-I (14). We (*25*, *27*) and others (*50*, *55*) have previously proposed that initial binding to lipid occurs via the association with lipid of the flexible carboxy-terminal region of the protein. With this in mind, the earliest possible intermediate proceeding from species B is represented by species C. A later intermediate, species D, is proposed based on the present studies of apo Δ(1−65)A-I(+his). Conversion to intermediate D proceeds through a conformational switch in amino-terminal residues 1−43 (previously suggested in ref *25*) that unmasks a latent lipid-binding domain, proposed here to be minimally formed by helix 1 (residues 44−65). The final lipid-bound conformation, represented by discoidal rLp2A-I, is supported by our published crystal structure of apo Δ(1−43)A-I, which shows the protein is a ring-shaped continuous helix (*24*). In light of this structure, it seems reasonable and most conservative to propose the protein wraps around the disk while maintaining the conformation shown in intermediate D. The protein is presented in both a hairpin, "closed belt" conformation, which requires little structural rearrangement from intermediate D, and an antiparallel, "open belt" conformation, which more closely mimics the crystal structure of apo Δ(1−43)A-I, an open, elliptical ring of antiparallel dimers. The latter conformation can be envisaged to proceed from intermediate D by an "unzipping" mechanism which would conservatively convert hydrophobic helix−helix interactions within the protein to hydrophobic interactions between the helices and the lipid. While the general principles presented in this lipid-binding mechanism are consistent with several lipid-bound conformations, we suggest that the helices bind such that they are perpendicular to the acyl chains of the lipid. The "belt" model for discoidal lipoproteins has been proposed for two other apolipoproteins; apolipoprotein E (*56*) and apolipophorin III (*57*, *58*) as well as a synthetic peptide from apo hA-I [residues 122−187 (*59*)]. Further studies with other mutants should provide additional details to this model.

ACKNOWLEDGMENT

We would like to thank Rodney Ott for his experience with the model XLA ultracentrifuge.

REFERENCES

1. Segrest, J. P., Jones, M. K., DeLoff, H., Brouillette, C. G., Venkatachalapathi, Y. V., and Anantharamaiah, G. M. (1992) *J. Lipid Res. 33*, 141−166.
2. Brouillette, C. G., and Anantharamaiah, G. M. (1995) *Biochim. Biophys. Acta 1256*, 103−129.
3. Fielding, C. J., and Fielding P. E. (1995) *J. Lipid Res. 36*, 211−228.
4. Barter, P. J., and Rye, K.-A. (1996) *Atherosclerosis 121*, 1−12.
5. Andersson, L. (1997) *Curr. Opin. Lipidol. 8*, 225−228.
6. Calabresi, L., and Franceschini, G. (1997) *Curr. Opin. Lipidol. 8*, 219−224.
7. Glomset, J. A. (1968) *J. Lipid Res. 9*, 155−167.
8. Blackburn, W. D., Jr., Dohlman, J. G., Venkatachalapathi, Y. V., Pillion D. J., Koopman, W. J., Segrest, J. P., and Anantharamaiah, G. M. (1991) *J. Lipid Res. 32*, 1911−1918.
9. Tytler, E. M., Segrest, J. P., Epand, R. M., Nie, S.-Q., Epand, R. F., Mishra, V. K., Venkatachalapathi, Y. V., and Anantharamaiah, G. M. (1993) *J. Biol. Chem. 268*, 22112−22118.
10. Owens, R. J., Anantharamaiah, G. M., Kahlon, J. B., Srinivas, R. V., Compans, R. W., and Segrest, J. P. (1990) *J. Clin. Invest. 86*, 1142−1150.
11. Srinivas, R. V., Birkedel, B., Owens, R. J., Anantharamaiah, G. M., Segrest, J. P., and Compans, R. W. (1990) *Virology 176*, 48−57.
12. Levine, D. M., Parker, T. S., Donnelly, T. M., Walsh, A., and Rukbin, A. L. (1993) *Proc. Natl. Acad. Sci. U.S.A. 90*, 12040−12044.
13. Sviridov, D., Pyle, L., and Fidge, N. (1996) *Biochemistry 35*, 189−196.
14. Bergeron, J., Frank, P. G., Emmanuel., F., Latta, M., Zhao, Y., Sparks, D. L., Rassart, E., Denefle, P., and Marcel, Y. L. (1997) *Biochim. Biophys. Acta 1344*, 139−152.
15. Schmidt, H. H.-J., Remaley, A. T., Stonik, J. A., Ronan, R., Wellmann, A., Thomas, F., Zech, L. A., Brewer, H. B., Jr., and Hoeg, J. M. (1995) *J. Biol. Chem. 270*, 5469−5475.
16. Frank, P., Bergeron, J., Emmanuel, F., Lavigne, J., Sparks, D., Denèfle, P., Rassart, E., and Marcel Y (1997) *Biochemistry 36*, 1798−1806.
17. Dhoest, A., Zhao, Z., Geest, B., Deridder, E., Sillen, A., Engelborghs, Y., Collen, D., and Holvoet, P. (1997) *J. Biol. Chem. 272*, 15967−15972.
18. Laccotripe, M., Makrides, S., Jonas, A., and Zannis, V. (1997) *J. Biol. Chem. 272*, 17511−17522.
19. Davidson, W. S., Hazlett, T., Mantulin, W. M., and Jonas, A. (1996) *Proc. Natl. Acad. Sci. U.S.A. 93*, 13605−13610.
20. Holvoet, P., Zhao, Z., Vanloo, B., Vos, R., Deridder, E., Shoest, A., Taveirne, J., Brouwers, E., Demarsin, E., Engelborghs, Y., Rosseneu, M., Collen, D., and Brasseur, R. (1995) *Biochemistry 34*, 13334−13342.
21. Minnich, A., Collet, X., Roghani, A., Cladaras, C., Hamilton, R. L., Fielding, C. J., and Zannis, V. I. (1992) *J. Biol. Chem. 267*, 16553−16560.
22. Sorci-Thomas, M., Kearns, M. W., and Lee, J. P. (1993) *J. Biol. Chem. 268*, 21403-21409.
23. Sorci-Thomas, M., Curtiss, L., Parks, J. S., Thomas, M. J., and Kearns, M. W. (1997) *J. Biol. Chem. 272*, 7278−7284.
24. Borhani, D. W., Rogers, D. P., Engler, J. A., and Brouillette, C. G. (1997) *Proc. Nat. Acad. Sci. U.S.A. 94*, 12291−12296.
25. Rogers, D. P., Brouillette, C. G., Engler, J. A., Tenidan, S. W., Roberts, L., Mishra, V. K., Anantharamaiah, G. M., Lund-Katz, S., Phillips, M. C., and Ray, M. J. (1997) *Biochemistry 36*, 288−300.

26. Rogers, D. P., Roberts, L., Lebowicz, J., Engler, J. A., and Brouillette, C. G. (1998) *Biochemistry 37*, 945−955.
27. Roberts, L. M., Ray, M. J., Shih, T., Hayden, E., Reader, M. M., and Brouillette, C. G. (1997) *Biochemistry 36*, 7615−7624.
28. Anantharamaiah, G. M., Hughes, T. A., Iqbal, M., Gawish, A., Neame, P. J., Medley, M. F., and Segrest, J. P. (1988) *J. Lipid Res. 29*, 309−318.
29. Hughes, T. A., Moore, M. A., Neame, P., Medley, M. F., and Chung, B. H. (1988) *J. Lipid Res. 29*, 362−376.
30. Pownall, H. J., and Massey, J. B. (1986) *Methods Enzymol. 128*, 515−518.
31. Cheung, P., and Chan, L. (1983) *Nucleic Acids Res. 11*, 3703−3715.
32. Vieira, J., and Messing, J. (1987) *Methods Enzymol. 153*, 3−12.
33. Zoller, M. J., and Smith, M. (1983) *Methods Enzymol. 100*, 468.
34. Studier, F. W., and Moffat, B. A. (1986) *J. Mol. Biol. 189*, 113.
35. Albers, J. J., Chken, C. H., and Lacko, A., G. (1986) *Methods Enzymol. 129*, 763−783.
36. Anantharamaiah, G. M., Venkatachalapathi, Y. V., Brouillette, C. G., and Segrest, J. P. (1990) *Arteriosclerosis 10*, 95−105.
37. Spuhler, P., Anantharamaiah, G. M., Segrest, J. P., and Seelig, J. (1994) *J. Biol. Chem. 269*, 23904−23910.
38. Pownall, H. J., Massey, J. B., Kusserow, S. K., and Gotto, A. M., Jr. (1978) *Biochemistry 17*, 1183−1188.
39. Lebowitz, J., Kar, S., Braswell, E., McPherson, S., and Richard, D. L. (1994) *Protein Sci. 3*, 1374−1382.
40. Aggerbeck, L. P., Wetterau, J. R., Weisgraber, K. H., Wu, C.-S. C., and Lindgren, F. T. (1988) *J. Biol. Chem. 263*, 6249−6258.
41. Barbeau, D. L., Jonas, A., Teng, T., and Scanu, A. M. (1979) *Biochemistry 18*, 362−369.
42. Laue, T. M., Shah, B. D., Ridgeway, T. M., Pelletier, S. L. (1992) *Analytical Ultracentrifugation in Biochemistry and Polymer Science*, pp 90−125, Royal Society of Chemistry, Cambridge, U.K.
43. Cantor, C. R., and Schimmel, P. R. (1980) *Biophysical Chemistry*, Vol. 2, p 161, Freeman, San Fransciso, CA.
44. Van Holde, and Weischet (1978) *Biopolymers 17*, 1387−1403.
45. Hansen, J. C., Lebowitz, J., and Demeler, B. (1994) *Biochemistry 33*, 13155−13163.
46. Tendian, S. W., Myszka, D. G., Sweet, R. W., Chaiken, I. M., and Brouillette, C. G. (1995) *Biochemistry 34*, 6464−6474.
47. Chen, Y.-H., Yang, J. T., and Martinez, H. M. (1972) *Biochemistry 11*, 4120−4131.
48. Sorci-Thomas, M., Parks, J. P., Kearns, M. W., Pate, G. N., Zhang, C., and Thomas, M. J. (1996) *J. Lipid Res. 37*, 673−683.
49. McGuire, K. A., Davidson, W. S., and Jonas, A. (1996) *J. Lipid Res. 37*, 1519−1528.
50. Ji, Y., and Jonas, A. (1995) *J. Biol. Chem. 270*, 11290−11297.
51. Goto, Y., and Fink, A. L. (1989) *Biochemistry 28*, 945−952.
52. Stryer, L. (1965) *J. Mol. Biol. 13*, 482−495.
53. Semisotnov, G. V., Rodionova, N. A., Kutyshenko, V. P., Ebert, B., Blanck, J., and Ptitsyn, O. B. (1987) *FEBS Lett. 224*, 9−13.
54. Palgunachari, M. N., Mishra, V. K., Lund-Katz, S., Phillips, M. C., Adeyeye, S. O., Alluri, S., Anantharamaiah, G. M., and Segrest, J. P. (1996) *Arterioscler. Thromb. 16*, 328−338.
55. Nolte, R. T., and Atkinson, D. A. (1992) *Biophys. J. 63*, 1221−1239.
56. Small, D. (1993) Determination of HDL structures. in *Atherosclerosis Reviews* (1993) (Catapano, A., Bernini, F., and Corsini, A., Eds.) Vol. 24, pp 1−15, Raven Press, New York.
57. Raussens, V., Narayanaswami, V., Goormaghtigh, E., Ryan, R. O., and Ruysschaert, J.-M. (1995) *J. Biol. Chem. 270*, 12542−12547.
58. Raussens, V., Narayanaswami, V., Goormaghtigh, E., Ryan, R. O., and Ruysschaert, J.-M. (1995) *J. Biol. Chem. 271*, 23089−23095.
59. Wang, G., Sparrow, J. T., and Cushley, R. J. (1997) *Biochemistry 36*, 13657−13666.
60. Edelstein, C., and Scanu, A. M. (1980) *J. Biol. Chem. 255*, 5747−5754.
61. Cohn, E. J., and Edsall, J. T. (1943) *Proteins, Amino Acids and Peptides as Ions and Dipolar Ions*, pp 370−381, Reinhold, New York.

BI973112K